Journal of Structural Geology 94 (2017) 154–165

Contents lists available at ScienceDirect

Journal of Structural Geology

journal homepage: www.elsevier.com/locate/jsg

Frictional behaviour of sandstone: A sample-size dependent triaxial investigation

Hamid Roshan [a, *], Hossein Masoumi [b], Klaus Regenauer-Lieb [a]

[a] School of Petroleum Engineering, UNSW Australia, Sydney, NSW, 2052, Australia
[b] School of Mining Engineering, UNSW Australia, Sydney, NSW, 2052, Australia

ARTICLE INFO

Article history:
Received 12 February 2016
Received in revised form
22 November 2016
Accepted 30 November 2016
Available online 1 December 2016

Keywords:
Size effect
Friction coefficient
Brittleness
Ductility
Thermodynamics

ABSTRACT

Frictional behaviour of rocks from the initial stage of loading to final shear displacement along the formed shear plane has been widely investigated in the past. However the effect of sample size on such frictional behaviour has not attracted much attention. This is mainly related to the limitations in rock testing facilities as well as the complex mechanisms involved in sample-size dependent frictional behaviour of rocks.

In this study, a suite of advanced triaxial experiments was performed on Gosford sandstone samples at different sizes and confining pressures. The post-peak response of the rock along the formed shear plane has been captured for the analysis with particular interest in sample-size dependency. Several important phenomena have been observed from the results of this study: a) the rate of transition from brittleness to ductility in rock is sample-size dependent where the relatively smaller samples showed faster transition toward ductility at any confining pressure; b) the sample size influences the angle of formed shear band and c) the friction coefficient of the formed shear plane is sample-size dependent where the relatively smaller sample exhibits lower friction coefficient compared to larger samples.

We interpret our results in terms of a thermodynamics approach in which the frictional properties for finite deformation are viewed as encompassing a multitude of ephemeral slipping surfaces prior to the formation of the through going fracture. The final fracture itself is seen as a result of the self-organisation of a sufficiently large ensemble of micro-slip surfaces and therefore consistent in terms of the theory of thermodynamics. This assumption vindicates the use of classical rock mechanics experiments to constrain failure of pressure sensitive rocks and the future imaging of these micro-slips opens an exciting path for research in rock failure mechanisms.

1. Introduction

Triaxial experiments are used to characterize and quantify the mechanical response of materials under simulated in-situ conditions (Bésuelle et al., 2000; Chang and Jumper, 1978; Khan et al., 1991, 1992; Klein et al., 2001; Niandou et al., 1997; Parry, 1960; Sulem and Ouffroukh, 2006a; Wasantha et al., 2014).

Little emphasis however has been placed on the size effect of the triaxial response of the investigated materials. Size effects are particularly pronounced for geological loading conditions where the behaviour of a sample from initial stage of loading to shear displacement along formed shear plane at different confining pressures is of interest. Size effects have been demonstrated under different loading/stress conditions including uniaxial compressive test (Baecher and Einstein, 1981; Darlington and Ranjith, 2011; Masoumi et al., 2014; Mogi, 1962; Panek and Fannon, 1992; Pratt et al., 1972; Thuro et al., 2001a), point load test (Broch and Franklin, 1972; Brook, 1980; Forbes et al., 2015; Greminger, 1982; Hawkins, 1998; Thuro et al., 2001b) and indirect tensile or so called Brazilian test (Andreev, 1991a, b; Butenuth, 1997; Çanakcia and Pala, 2007; Carpinteri et al., 1995; Elices and Rocco, 1999; Thuro et al., 2001a). Also, a limited number of studies have included size effect under triaxial condition (Aubertin et al., 2000; Hunt, 1973; Medhurst and Brown, 1998; Singh and Huck, 1972) while neither has reported the full stress-strain response from the initial stage of loading to shear displacement beyond the peak

* Corresponding author.
E-mail address: h.roshan@unsw.edu.au (H. Roshan).

http://dx.doi.org/10.1016/j.jsg.2016.11.014
0191-8141/

stress. This has led to shortcoming in understanding of size effects on a) the rate of transition from brittle to ductile response, b) the formation of shear bands and c) the post-peak shear response along the formed shear plane particularly in sedimentary rocks.

Understanding the mechanisms involved in the transition from brittleness to ductility in sedimentary rocks is a vital aspect of the petroleum geomechanics, in particular reservoir production (Wong et al., 1997). In addition, the formation of shear band is of great interest in many disciplines from structural geology to petroleum geomechanics such as prediction of the fluid transmissivity along faults (Sulem and Ouffroukh, 2006b). Further, the friction coefficient of fractures is generally assumed size independent. However, a number of investigations have shown that the sample size influences the friction coefficient of rock discontinuities e.g. faults and fractures (Bandis, 1980; Bandis et al., 1981; Barton and Bandis, 1982; Carpinteri and Paggi, 2005; Schellart, 2000).

These investigations have proposed some form of descending size effect model for the friction coefficient. However, the studies were restricted to a statistical description and not aimed at gaining insight into the origins of the size effect. Consequently no universal law was derived and the proposed models did not seem to be able to suitably predict the sample-size dependent behaviour of the friction coefficient over the wide range of laboratory scales especially at relatively smaller sizes. A profound knowledge of the sample-size effect is particularly important in petroleum geomechanical projects where relatively small core samples are often retrieved from deep locations and available for the laboratory experiments.

In this study, a number of triaxial laboratory experiments were performed on Gosford sandstone samples at three different sample diameters with complete stress-strain behaviour from the initial stage of loading to shear displacement along the formed shear planes. Because of homogeneous porosity structure of Gosford Sandstone and its uniform mechanical response (Baud et al., 2000; Edmond and Paterson, 1972; Forbes et al., 2015; Masoumi et al., 2016; Ord et al., 1991; Roshan et al., 2016a; Sufian and Russell, 2013), it was used for a first systematic study to shed light on the origins and character of the sample-size effect for shear deformation. We present a first study that characterises the size effects on a) the rate of transition from brittle to ductile response in rock over a wide range of confining pressures, b) the formation of shear bands and c) the friction coefficient of the formed shear planes. We interpret the results by a novel thermodynamic homogenization approach (Regenauer-Lieb et al., 2014) using the upper bound method to derive a representative volume element for mechanical deformation of Gosford sandstone.

2. Sample preparation and experimental methodology

The laboratory triaxial experiments were conducted on Gosford sandstone samples with diameters of 25, 50 and 96 mm. Gosford sandstone forms a unit within the massive (290 m thick) Triassic Hawkesbury sandstone of the Sydney Basin (Ord et al., 1991) on the east coast of New South Wales, Australia (Fig. 1).

The Gosford sandstone used in this study was obtained from Gosford Quarry, Somersby, New South Wales, Australia. Samples were carefully selected to be as homogeneous as possible visually with no macro defect with a unified colour. Roshan et al. (2016b) conducted an X-ray computed tomography scan on the same batch of Gosford sandstone used in this study and reported its porosity to be approximately 16.0%. The maximum grain size of Gosford sandstone was estimated as 0.6 mm from sieve analysis. In addition, the mineralogy of the sample was measured as 86% quartz (SiO2), 7% illite (Al2 H2 K0.7 O12 Si4), 6%, kaolinite (H4 Al2 O9 Si2) and 1% anatase (TiO2) by X-ray diffraction analysis. All samples with length to diameter ratio of 2 (ASTM, 2000) were oven dried for 24 h at 105° C. To make the end surfaces flat, the cores were grounded carefully to about 0.003 mm tolerance according to ISRM (2007).

A servo-controlled loading frame system with maximum loading capacity of 300 tonnes was used to perform the triaxial experiments. A GCTS triaxial cell with the maximum axial loading capacity of 200 tonnes and 70 MPa confining pressure was employed (Fig. A1 in the Appendix). The triaxial cell came with three sets of platens at 100, 50 and 25 mm diameters. A manual hydraulic pump with maximum pressure capacity of 100 MPa was utilized to provide the confining pressure. An additional digital gauge manufactured by Geotechnical Digital Systems (GDS) with accuracy of ±0.01 MPa was used to control the confining pressure during the experiment. Two axial and one circumferential Linear Variable Differential Transducers (LVDT) were utilized to log the axial and radial deformations of the sample, respectively (Fig A2 in the Appendix). Subsequently the average of the axial deformations was used for data interpretation. Several experiments were conducted on each size (25, 50 and 96 mm) and confining pressure (10, 20 and 30 MPa) to account for possible scatters.

The deviatoric stress is defined as $q = \sigma_1 - \sigma_3$ where σ_3 is the confining pressure and σ_1 is the axial stress. The shear band angle (β) is referred to the angle between the formed shear plane and the horizon which is measured after complete failure of the sample. The residual deviatoric stress in the stress-strain curve is also referred to the final permanent deviatoric stress level, in which the shearing occurs along the shear plane with no change in the deviatoric stress.

3. Results

Examples of one set of conventional triaxial deviatoric stress (q) versus axial strain for 25, 50 and 96 mm diameter samples under three confining pressure (10, 20 and 30 MPa) are shown in Fig. 2. The mean peak and residual deviatoric stresses as well as the shear band angles (β) at different sizes and confining pressures are extracted from the experimental data and reported in Table 1.

Shear band angles were attained according to the method proposed by El Bied et al. (2002) where attempts were made to conduct the measurement at the centre of the shear plane to minimise the effect of deviated shear angles close to the end surfaces. The measured shear band angles at different confining pressures for all three diameters are presented in Fig. 3. The photos of the formed shear bands for a set of triaxial tests on each sample size at different confinements are additionally presented in Appendix (Figs. A3-A5).

Fig. 3 shows that an increase in confining pressure leads to decrease in shear band angle for all three diameters with different degree of sample-size dependency. The data obtained from triaxial testing at different sample sizes are used to investigate the effect of sample size on a) the rate of transition from brittle to ductile response, b) shear band angle, and c) the friction coefficient of formed fractures.

3.1. Sample-size effect on the rate of transition from brittleness to ductility

The mean peak and residual deviatoric stresses reported in Table 1 for 10, 20 and 30 MPa confining pressures are used to investigate the size effect on the rate of transition from brittle to ductile response e.g. ductile response is defined as where the incremental stress shows no softening with strain. A relationship, so called the transition index (TI), is defined to study this process:

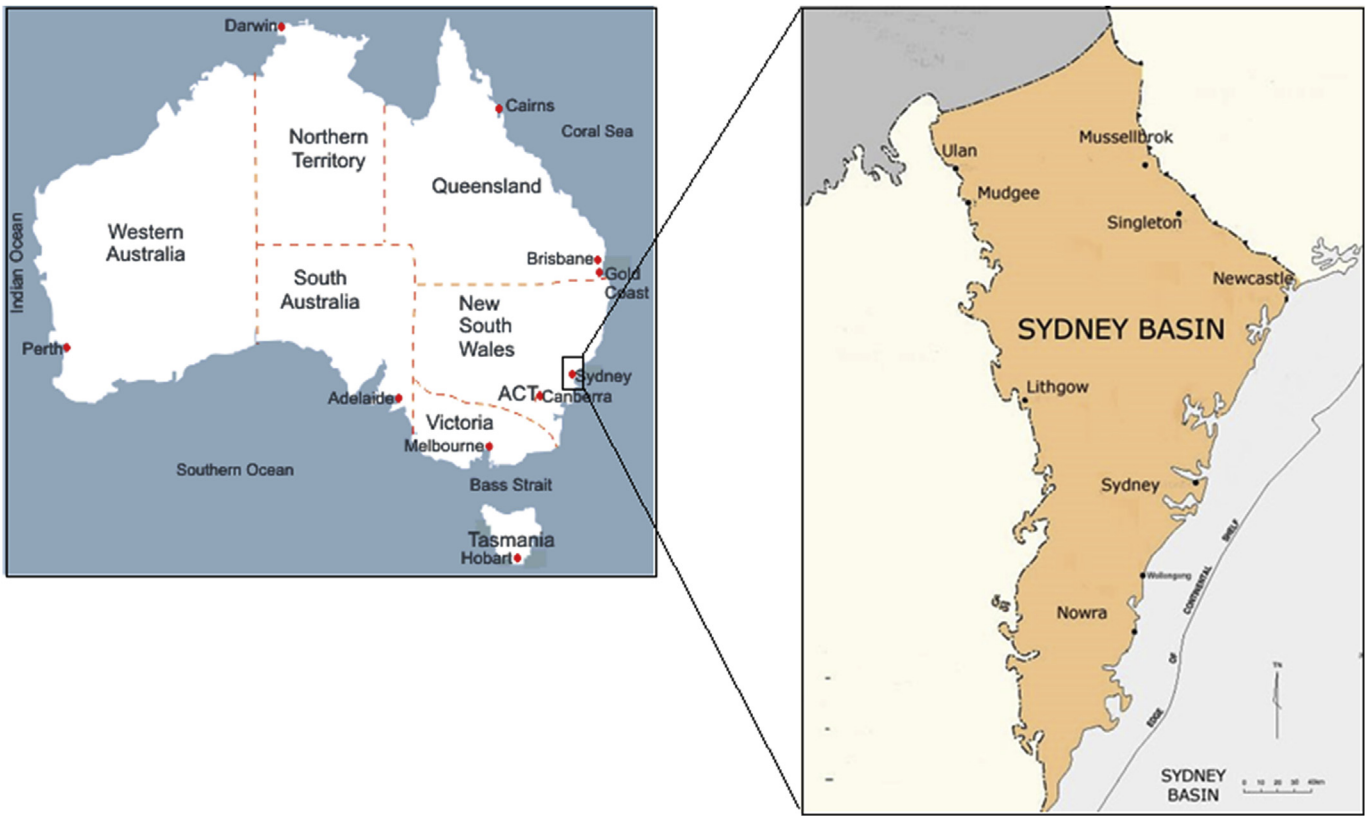

Fig. 1. Location map of Sydney Basin.

$$\mathrm{TI}=\frac{\text{Mean peak deviatoric stress}-\text{Mean residual deviatoric stress}}{\text{Mean peak deviatoric stress}}$$

From this definition, TI approaches one when the sample shows strong brittleness while for highly ductile rock, TI moves towards zero or negative values (with strain hardening). The trends of TI are calculated for three different sizes under different confinements and presented in Fig. 4. It is evident from Fig. 4 that the TI varies almost linearly with confining pressure for all three sample sizes where the level of ductility increases with an increase in confining pressure (Sulem and Ouffroukh, 2006b). Fig. 4 also indicates that the TI of the samples with 50 and 96 mm diameters are very close to each other at almost all confining pressures but considerably higher than that of 25 mm diameter samples. More importantly, Fig. 4 demonstrates that at each confining pressure, TI increases and then slightly decreases with an increase in sample size from 25 mm to 96 mm. The rate of TI reduction from 50 mm diameter to 25 mm diameter is more pronounced than that between 50 and 96 mm diameter. It has been widely reported (Brady and Brown, 2006; Elliot and Brown, 1985; Mogi, 1966; Wawersik and Fairhurst, 1970) that rocks show transition from brittle to ductile behaviour with an increase in confining pressure. Such a behaviour has been linked mainly to the closure of non-critical micro-fractures (Mogi, 1966) as confining pressure increases. It is also noted that the ductile response at relatively high confining pressure might be associated with crystalline plasticity, diffusional mass transfer or cataclastic flow (Baud et al., 2015; Wong and Baud, 2012). While the effect of confining pressure on the transition from brittleness to ductility of geo-materials has been widely investigated, no study has been investigated the influence of sample size on such transition. Interestingly, the results presented in Fig. 4 show that the samples with 25 mm diameter exhibit faster transition to ductile regime in comparison with the larger samples over the same range of confining pressures. In order to analyse the results more effectively, the mean value of the peak deviatoric stress was plotted versus sample diameter for three confining pressures of 10, 20 and 30 MPa (Fig. 5).

Roshan et al. (2016a) carried out a size effect study on the uniaxial compressive strength (UCS) of several sedimentary intact rocks and reported an ascending-descending behaviour for UCS data. From Fig. 5, it is seen that the triaxial results also follow an ascending-descending behaviour similar to UCS data. Although only three sample sizes have been tested (due to limited number of platens), a clear sample-size dependency of triaxial results with ascending-descending behaviour is observed from Fig. 5.

As mentioned, above TI was defined by the difference between the peak and residual deviatoric stresses. The peak deviatoric stresses are sample-size dependent with ascending-descending trend (Fig. 5) while the residual deviatoric stresses are size independent (Table 1). Thus, TI follows the same trend as that shown for the peak deviatoric stresses (Fig. 5) which means TI increases with an increase in sample size at each confining pressure but starts reducing after reaching a characteristic diameter (here approximately 50 mm). In other words, at the same confining pressure, with an increase in sample size up to a characteristic diameter the level of brittleness increases and then above this characteristic diameter the level of brittleness reduces (ductility increases) as the sample size increases.

3.2. Sample-size effects on the shear band angle

The sample-size effect on the formation of the shear planes is also a key parameter in triaxial compression testing of

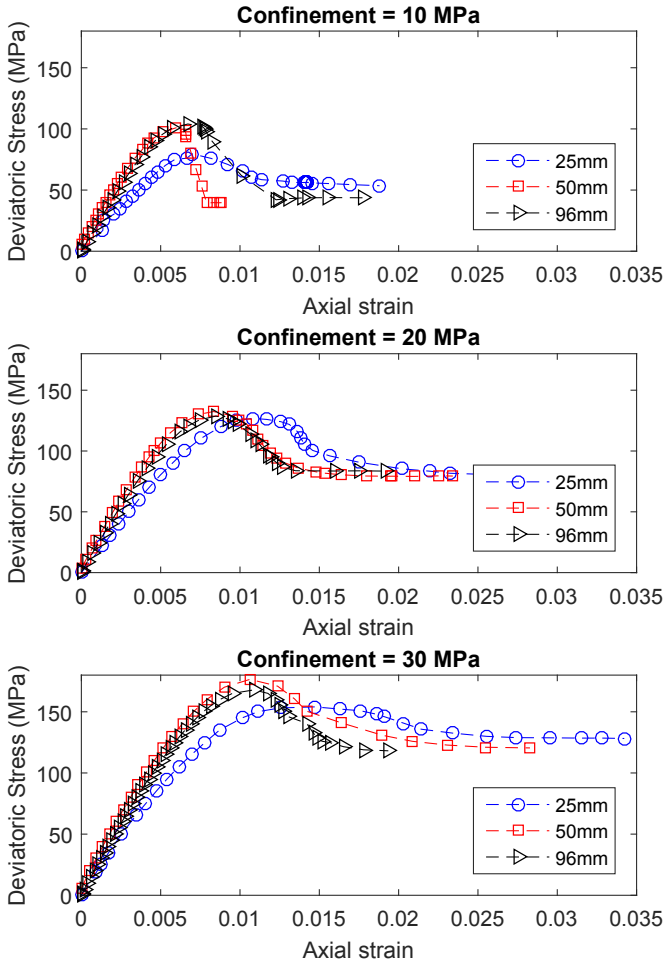

Fig. 2. Example of the triaxial stress-strain results for the samples with a) 25 mm, b) 50 mm and c) 96 mm diameters under three confinements: 10, 20 and 30 MPa.

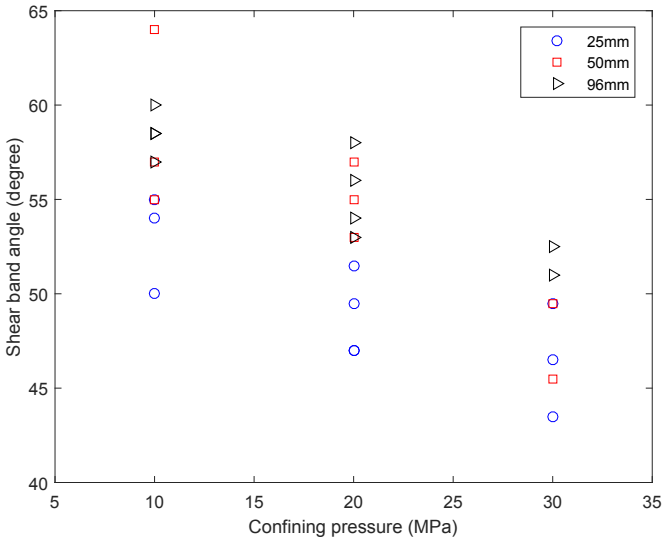

Fig. 3. The shear band angle versus confining pressure for samples with three different diameters: 25, 50 and 96 mm.

geomaterials. The trends of mean shear band angle versus confining pressure for samples having 25, 50 and 96 mm diameter are illustrated in Fig. 6.

From Fig. 6 it is observed that the shear band angle decreases with an increase in confinement for all three sample diameters. This is in agreement with the previously reported results (Bésuelle et al., 2000; El Bied et al., 2002) in which an increase in confining pressure leads to decrease in shear band angle. Maurer (1965) suggested that decrease in the shear band angle due to the confining pressure is associated with increase in sample ductility. Maurer (1965) argued that an increase in confining pressure leads to higher ductility which causes the sample to undergo large displacement. Such larger displacement mobilises the shear plane towards the horizon and consequently shear plane angle reduces (moving toward compaction bands). More interestingly, the shear band angles obtained from 25 mm diameter sample stay lower than those measured from 50 to 96 mm diameters (Fig. 6). The measured shear band angles for 50 and 96 mm diameter samples are very close to each other and follow a very similar trend to that of TI (Fig. 4).

3.3. Sample-size effect on the friction coefficient of the formed fracture

Efforts have been made in the past to study the sample-size effect on the friction coefficient of fractures and faults and relate it to field settings (Bandis, 1980; Bandis et al., 1981; Barton and Bandis, 1982; Carpenter et al., 2011, 2015; Carpinteri and Paggi, 2005; Schellart, 2000). The experimental work in this area,

Table 1
The mean peak and residual deviatoric stresses as well as the mean shear band angles obtained from Gosford sandstone at different sizes and confining pressures.

Confining pressure (MPa)	Mean peak deviatoric stress (MPa)	Mean residual deviatoric stress (MPa)	Mean shear band angle (β)
96 mm diameter			
10	105.6	44	58
20	134.1	80.5	55.5
30	169.1	122	51.5
50 mm diameter			
10	109.9	44	59.5
20	135.6	79	55.5
30	172.4	123	52.5
25 mm diameter			
10	96.7	45.0	52.5
20	127.2	80.2	47.5
30	154.5	122.9	45.5

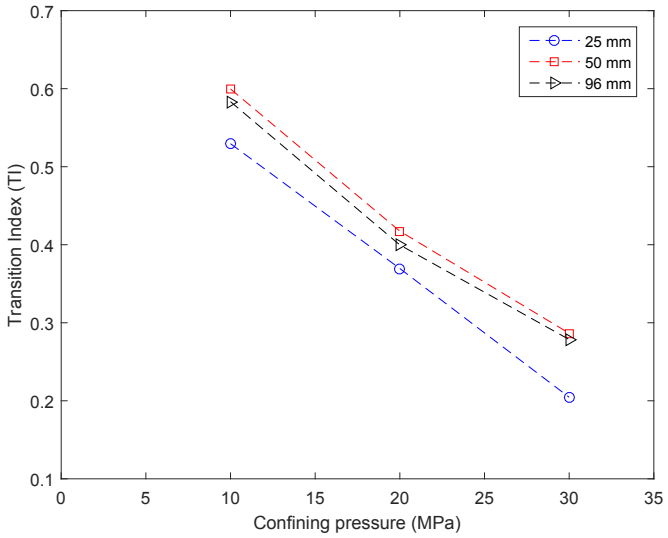

Fig. 4. Transition Index (*TI*) versus confining pressure for three sample sizes.

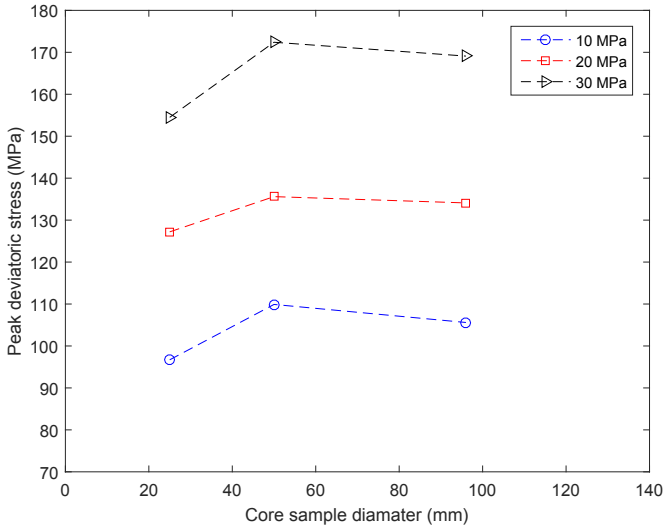

Fig. 5. Peak deviatoric stress versus sample diameter at different confining pressures.

however; has been often conducted on artificial fractures made within the intact rock by saw cutting (Byerlee, 1967, 1978; Kohli and Zoback, 2013). This can be representative of a fault at the late stage of growth where for instance considerable amount of gouge is present (Crider and Peacock, 2004). The artificial fractures however do not necessarily replicate the early stage of the brittle fault formation under shear forces near the crust (Crider and Peacock, 2004). In an early study, Byerlee (1967) investigated this phenomenon by comparing the frictional behaviour of three different samples including an intact granite, a granite with natural fracture and a granite with artificial fracture. Byerlee (1967) showed that while the frictional behaviour of the naturally and artificially fractured granites are very similar, their behaviours are quite different to that of intact granite, fractured under triaxial condition. Therefore, those faults which form under progressive initial shear failure are best represented by the triaxial experiment on an intact rock. In

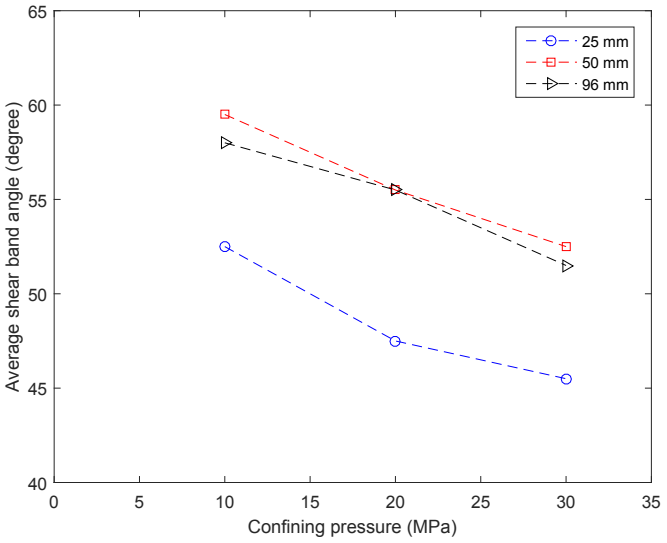

Fig. 6. The mean angle of the formed shear bands versus confining pressure for different sample sizes.

triaxial testing, the shear (τ) and normal (σ_n) stresses on the shear plane are calculated from the shear band angle (β), deviatoric stress (q) and confining pressure (σ_3)

$$\sigma_n = \frac{(q+2\sigma_3)}{2} + \frac{q}{2}\cos 2\beta \quad (1)$$

$$\tau = \frac{q}{2}\sin 2\beta \quad (2)$$

It is known that the formation of the shear bands initiates before reaching the peak deviatoric stress (Ord et al., 2007) and then grows to form the macro shear plane after peak stress. From peak stress onward during the softening stage rock will experience disintegration towards the residual stress (Byerlee, 1967). This is followed by a shear displacement along the formed shear plane at a constant residual stress (Bésuelle et al., 2000). Overall, such a behaviour is very similar to a simple shear test on a jointed rock where the stress (or force) increases up to the peak point and then decreases to the residual stress (Bandis et al., 1981; Byerlee, 1978) (Fig. 7). Therefore, it seems important to report the friction coefficients at both peak and

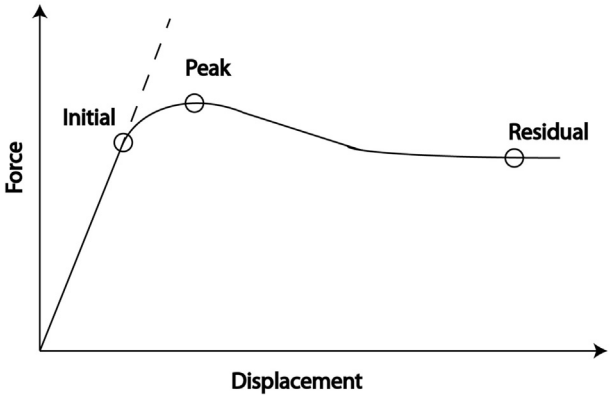

Fig. 7. Schematic representation of the force versus displacement from a triaxial test on an intact rock or direct shear test on a jointed rock.

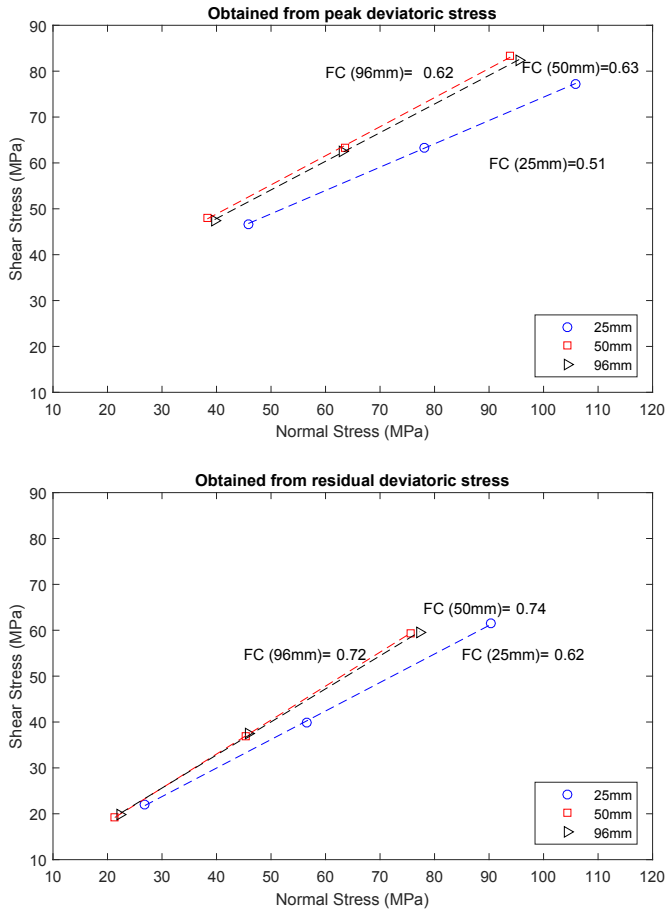

Fig. 8. Shear stress versus normal stress along the shear plane extracted from a) the peak deviatoric stresses and confining pressures and b) the residual deviatoric stresses and confining pressures for different sample diameters.

residual stresses as highlighted by Byerlee (1978). The shear and normal stresses are thus extracted from the peak and residual stresses at different sizes and plotted in Fig. 8.

It is evident from Fig. 8 that the friction coefficients obtained from both the peak and residual deviatoric stresses are sample-size dependent. At peak stress, both the peak deviatoric stress and shear band angle contribute to sample-size dependency of the friction coefficient as they are both sample-size dependent. On the other hand, at residual stress, only the sample-size dependency of the shear band angle causes the friction coefficient to be sample-size dependent. Consequently, the friction coefficients obtained from the peak stresses are: 0.51, 0.63 and 0.62 for 25, 50 and 96 mm diameter samples respectively and 0.62, 0.74 and 0.72 for 25, 50 and 96 mm diameter samples from residual stresses.

It was previously mentioned that the effect of size on peak stress and shear plane angle lead to sample-size dependency of the friction coefficients at the peak stress. It was also discussed that the peak stress in particular poses an ascending-descending behaviour (Fig. 6). Therefore, it is logical to expect that the friction coefficient in turn follows an ascending-descending trend similar to that reported for peak stresses. In fact, with an increase in sample size up to a characteristic diameter, the friction coefficient increases and then above this characteristic diameter the friction coefficient reduces with sample size. Several studies have reported the descending behaviour for friction coefficient with increase in sample size (Bahaaddini et al., 2014; Bandis et al., 1981; Barton and Bandis, 1982) which is in agreement with the observed friction coefficients of this study within the descending zone.

4. Discussion

The theory of thermodynamics allows for the development of a fundamental physics-based averaging technique (Regenauer-Lieb et al., 2014), which was shown to be robust for both far from equilibrium dynamic processes as well as for thermodynamic equilibrium (Roshan and Oeser, 2012; Regenauer-Lieb et al., 2013a, 2013b). The technique has proven particularly useful for the estimation of static and dynamic rock properties derived from micro-CT scans of core samples (Liu et al., 2015). Here we propose the theory as a potential exploration of the size effect of rock mechanical behaviour, in particular friction coefficients.

4.1. Thermodynamic bounds of a deformation process

Entropy production is a powerful abstraction tool for quantification and characterization of complex multi-scale processes. It provides a very high level of description by encapsulating not only the conditions of equilibrium of mass and momenta but also the principle of energy conservation. Entropy production can be directly related to the dissipation caused by irreversible processes plus the exchange of entropy with the surroundings. Dissipation is defined by the product of a thermodynamic force (e.g. difference in temperature, pressure, shear stress, chemical potentials, electrical potential, etc) times the thermodynamic flux (change in heat, volumetric strain rate, shear strain rate, chemical species, electrical current, etc). These dissipation processes phenomena are subject to a diffusion transport process that from a macroscopic point of view can often be described empirically by a diffusion equation (Fourier, Darcy, Fick, Ohm etc.). Characterizing the dissipation of a process such as the pressure sensitive yield of Gosford sandstone can be done from two different perspectives (Veveakis and Regenauer-Lieb, 2015b).

4.1.1. Upper bound (constant thermodynamic flux boundary condition)

Classical geomechanical approaches traditionally use an upper bound and thus enforce the principle of maximum dissipation. This represents a restriction of the second law of thermodynamics to the strong form, which can only be applied to the macroscopic limit of material behaviour, if it exists. In other words classical geomechanics approaches assume that the thermodynamic averaging of the considered volume element is large enough and the deformation process has proceeded for a sufficient length of time that it can be considered a time-independent (steady state) process. The upper bound provides a macroscopic perspective of the deformation process.

4.1.2. Lower bound (constant thermodynamic force boundary condition)

A lower bound of dissipation can be calculated when considering an explicit formulation of micro-processes that can locally under special conditions violate the theory of thermodynamics (i.e. produce negative entropy). In this case statistical mechanics must be used to evaluate the microscopic interactions. When a sufficiently large volume element is considered the theory of finite time thermodynamics can be applied (Andresen and Salamon 1984) and we can evaluate a lower bound of entropy production. The finite

time thermodynamics lower bound assesses the energetics of an assembly of micro-processes where time plays a significant role. The lower bound provides a microscopic time-dependent perspective of the deformation process.

4.2. Two scales of thermodynamic homogenization

When evaluating a dynamic process such as the finite deformation of rock samples the first point to consider is whether the sampling volume considered suffices the minimum requirement to satisfy the theory of thermodynamics. In other words the number of micro-processes over which the thermodynamic averaging is performed must be sufficiently large such that it provides a suitable average of the entropy production of the micro-processes. This entropy production of the micro-processes can be evaluated by multiplying the thermodynamic flux by the thermodynamic force e.g. for the case of size effect on friction, it is the velocity of slip multiplied by the force applied to the slipping surface.

We identify two different scales of micro-processes for the frictional deformation of sandstone: the grain-grain contact across a slipping surface and the slipping surface itself. While the multitude of grain-grain contacts in Gosford sandstone most likely warrants the use of a thermodynamic approach (we will come to the scaling length later) the low number of slipping surfaces (usually a single fracture) as the outcome of the experiment does not warrant a thermodynamic approach. This would imply that the outcomes of a rock mechanics experiment, as performed here, are not suitable for the use of classical continuum geomechanics theories as the continuum assumption is only fulfilled for averaging grain-grain contact for frictional behaviour on a pre-cut surface but not for the formation of a few slipping surfaces. The outcomes of the friction experiment performed here would have to be interpreted by statistical mechanics considering the interaction of the few failure surfaces with the testing machine. This would involve a detailed assessment of the elastic energy stored in the testing machine and the sample, the geometry and frictional condition of contact between testing machine and sample, the sample dimensions, aspect ratio, loading rate, confining medium etc. The results of our experiment would be variable and a function of all these statistical mechanics elements and, hence be highly variable for deriving frictional properties for continuum mechanics.

The success of continuum rock mechanics and the many practical uses of rock mechanics experiments for field conditions belie the conclusion drawn from this line of arguments. As a way out we postulate here the existence of a thermodynamic continuum leading to the formation of the main fracture(s). The frictional properties for finite deformation of Gosford sandstone could then be estimated using the upper bound approach assuming that the volume element must be large enough to encompass a multitude of ephemeral slipping surfaces (shear bands) prior to the formation of the through going fracture. The final fracture itself is seen as a result of the self-organisation of a sufficiently large ensemble of micro-slip surfaces and therefore consistent in terms of the theory of thermodynamics. Although the existence of multiple slip surfaces is well known by experimentalist, the suggested precursory phenomenon is not well documented. In order to conclusively prove this postulate we would need high-resolution time-lapse deformation experiments done in Synchrotron X-Ray CT to be able to resolve this extremely fast process. Unfortunately such experiments are not yet available.

Several attempts however have been made to characterize this phenomenon. Desrues and Andò (2015) used Micro CT scanning to investigate the formation of shear bands. They discussed that the displacement and rotation of individual grains with respect to their neighbours play major role in kinetics of shear band and it was concluded that the shear band forms before peak stress. In another study, Brantut et al. (2014) investigated the link between the microscale crack growth and macroscopic rate dependency and clear relationship was evident.

For lack of complete laboratory evidence we have to resort to numerical experiments using digital rock equivalents. Particle Flow Code Simulations (PFC) using the statistical mechanics approach of contact laws between grains have clearly shown a precursor phenomenon of coordinated particle movements prior to the emergence of a macroscopic shear band (Durrleman et al., 2006; Ord et al., 2007).

A characteristic scaling relationship of multiple slipping surfaces was also observed early on in numerical simulation of frictional deformation of rocks (Ord, 1990; Poliakov et al., 1994). These experiments were done without special attention to the intrinsic fundamental length scale governing the scaling relationship including the evolution from multiple slipping surfaces to a major localization band. A fundamental length scale for one particular micro-mechanism was later on shown to regularize the inherent mesh-sensitivity of these calculations by introducing an internal length scale (Regenauer-Lieb and Yuen, 2004). In this particular simulation the diffusional length scale was identified as the internal length scale. The diffusive length scale was explicitly calculated from the feedback phenomenon of ductile creep, shear heating and heat conduction and mesh sensitivity was avoided. The dynamic evolution of the shear bands was also investigated in Regenauer-Lieb and Yuen (2004). The calculations clearly illustrated how an ensemble of micro-shear bands self-organises around its lowest wavelength eigenmode and ultimately coalesces into a large-scale major shear surface. This finding would indeed verify the postulate that the theory of thermodynamics is fulfilled prior to the ultimate failure and therefore vindicate the use of rock mechanics experiments to constrain yield envelopes of pressure sensitive rocks. In order to generalise these findings from numerical experiments a sound brief theoretical derivation is required.

4.3. Theoretical derivation of the fundamental scales for the two scales of homogenization

4.3.1. Width of the shear band

For the small length-scale the thickness of a singular shear band in granular materials such as Gosford sandstone was developed by Mühlhaus and Vardoulakis (1987) as the first theoretical approach. Later on other theories and experiments have been used to verify the fundamental prediction that the shear bands have a finite width of the order of ten grain diameters (Francois et al., 2002). Based on these findings three different approaches were developed to introduce this fundamental length scale into continuum mechanics to regularize the mesh sensitivity of numerical solution by a physical mechanisms, these were: nonlocal elasticity, gradient elasticity and Cosserat elasticity (Francois et al., 2002). Although the width was found to naturally vary somewhat the approach has since been very successful to avoid mesh-sensitivity in microstructurally enriched continuum theories (Geers et al., 2010).

4.3.2. Distance between shear bands

While all Gosford sandstone samples contain many more than 1000 grains and satisfy the thermodynamic upper bound homogenization criterion this may not necessarily be the case for the

larger length scale, i.e. the distance between shear bands. This distance can be derived on the basis of a new finite time thermodynamic theory for the deformation of solids (Veveakis and Regenauer-Lieb, 2015a). In this "*Wave Mechanics*" theory (Regenauer-Lieb et al., 2016) deformational instabilities are interpreted as propagating elasto-plastic shock waves and decomposed into (S)-waves and (P)-waves that superpose. In the stationary limit, where the shock waves form standing stationary waves, they are equivalent to the localization features known from the classical continuum mechanics theory such as shear bands, dilation bands or compaction bands. In most cases the shear band (stationary (S) − wave) is the dominant feature but it can have some small volumetric deformation (stationary (P) − wave) superposed leading to differences in orientation of shear bands (Vermeer, 1990).

Of special interest for the distance between the shear bands is this small percentage of volumetric strain, which stems from the propagating pressure (P)-waves that in the stationary limit are called a cnoidal waves (Veveakis and Regenauer-Lieb, 2015a). This stationary limit is perfectly periodic and cnoidal waves are the solid-mechanical equivalent of standing wave in shallow water theory, forming sharp crests and long straight troughs. Since the elastic (P)- wave propagates ahead of the (S) − we argue that cnoidal waves form the seed for the ensemble of shear bands and dictate their distance. This characteristic scaling length is again a diffusive scaling length expressing the ratio of the compaction of the solid matrix over the capability of the air to diffuse out of the pore network via Darcy flow. The diffusive scaling length is δ_c:

$$\delta_c = \sqrt{\frac{k\mu_s}{\mu_f}} \tag{3}$$

whereby k is the permeability of Gosford sandstone, the viscosity of the solid matrix is $\mu_s = \frac{p}{\dot{\varepsilon}}$, p is the pressure of the (P-wave) and $\dot{\varepsilon}$ the volumetric strain rate. Although we are dealing with the Gosford sandstone case with a fluid (air) that has a low viscosity, μ_f it still plays a significant role in defining the distance between the shear bands. This relies on the fact that in order for the solid matrix to compact it must expel the air out of the reduced pore space. The exact values for the solid viscosity are unknown for Gosford sandstone, however, using this formula and available data from other sandstones the distance between the shear bands has been estimated to be on the order of mm to cm (Regenauer-Lieb et al., 2013b). If the distance for Gosford sandstone is several centimetres the above used sample size would be too small to reliably derive frictional properties from the rock mechanics experiments. Samples of the order of meter sizes would be required to satisfy the upper bound theorem.

4.4. Upper bound approach for frictional deformation of sandstone

We proceed by interpreting the size effect of our friction experiment in terms of the upper bound approach. In interpreting the results we use the expectations that for a larger sample size the dissipative property must converge to a lower value when using the upper bound approach as implied by a constant velocity boundary condition. This asymptotic homogenization method is well established in computational characterization of multi-scale systems (Terada et al., 2000) and is here applied for the first time for the interpretation of results from physical laboratory experiments.

In our experiments, we found an ascending-descending behaviour for the friction coefficient with increasing size. The ascending trend is definitely not what is expected from the upper bound approach and is strongly indicative of the sample being too small to be investigated by the upper bound approach for homogenization. Although the grain-grain contacts should average out in the upper bound approach and give scale invariant friction coefficients we argue that for the smaller samples the distance between the multiple shear bands is not very much smaller than the sample dimension, therefore prohibiting an upper bound approach for the sizes chosen. We conclude that the smaller sizes are unsuitable for the derivation of continuum mechanics properties e.g. where the fractal characteristics have been proposed as active mechanisms for strength ascending behaviour (Masoumi et al., 2016).

The descending trend is, however, consistent with the upper bound approach. Also the fact that the friction coefficients obtained from 50 to 96 mm diameter samples are much closer to each other than that of 25 mm diameter samples at both peak and residual stresses is encouraging. We conclude that the larger sample diameters can be interpreted with the upper bound approach and identify that the uncertainty for the 96 mm diameter sample is much smaller than that of the smaller samples. We also conclude that 96 mm is not a sufficiently large sample for reliable estimation of frictional properties of Gosford sandstone as the descending trend has not yet flattened out however the theory allows us to predict such stage through simulation.

5. Conclusion

A comprehensive sample-size dependent triaxial investigation was conducted on Gosford sandstone. The experiments covered the complete stress-strain behaviour from initial stage of loading to shear displacement along the formed shear plane.

From the results of this study, it was shown that the rate of transition from brittle to ductile behaviour at different confining pressures is a function of sample size. Such sample-size dependency exhibits an ascending-descending trend. This sample-size dependency was correlated with the rate of transition from brittleness to ductility of rock. It was also revealed that the shear band angle and friction coefficient of the formed shear planes are sample-size dependent.

The finding of this study is aligned with the postulate that the theory of thermodynamics is fulfilled prior to the ultimate failure and therefore vindicates the use of rock mechanics experiments to constrain yield envelopes of pressure sensitive rocks. The interpretation shows that the ascending trend is indicative of the sample being too small to follow the upper bound limit for homogenization. Although the grain-grain contacts should average out in the upper bound approach and give scale invariant friction coefficients we argue that for the smaller samples the distance between the multiple shear bands is not very much smaller than the sample dimension, therefore prohibiting an upper bound approach for relatively small sizes.

The descending trend is, however, consistent with the upper bound approach thus the larger sample diameters can be interpreted with the upper bound approach. As a result the uncertainty in measured friction coefficient for the 96 mm diameter sample is much smaller than that of the smaller samples. The final frictional properties of Gosford sandstone can be extracted when the descending trend has flattened out which can be predicted with the proposed theory through simulation.

Appendix

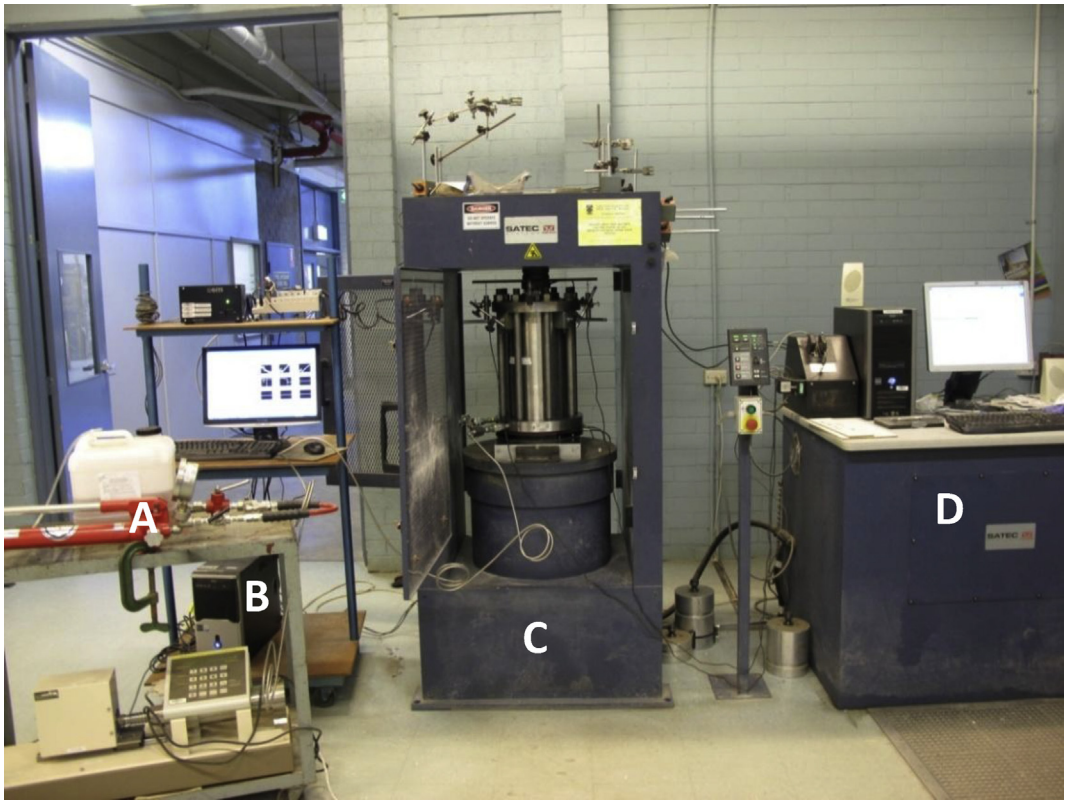

Fig. A1. Elements of the triaxial system: A- Hydraulic pump to provide and continuously control the confining pressure (± 0.01 MPa), B- Computer system for data acquisition, C- Loading frame and D- The loading frame control system.

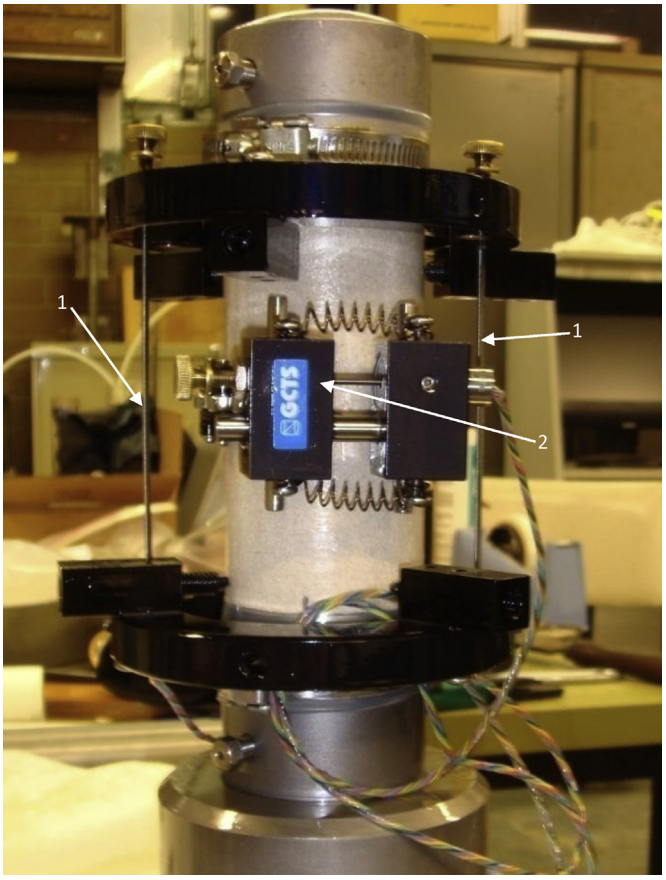

Fig. A2. (1) Two axial LVDTs were held by the top and lower rings and the rings were bolted to the 50 mm diameter sample over the membrane. (2) Circumferential LVDT attached to the sample using a spring chain.

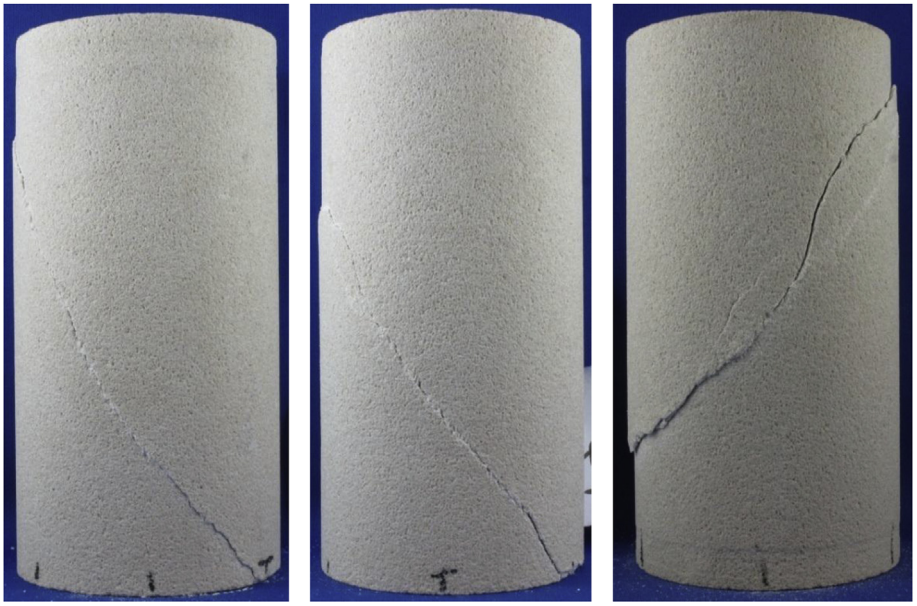

a) 10MPa b) 20MPa c) 30MPa

Fig. A3. Typical fracture patterns resulted from triaxial tests on 96 mm diameter samples at different confining pressures.

a) 10MPa b) 20MPa c) 30MPa

Fig. A4. Typical fracture patterns resulted from triaxial tests on 50 mm diameter samples at different confining pressures.

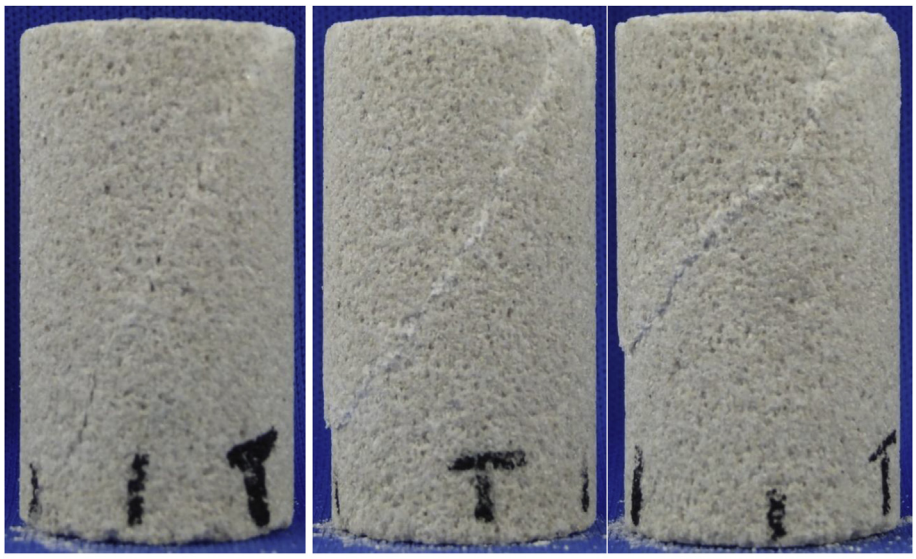

a) 10MPa b) 20MPa c) 20MPa

Fig. A5. Typical fracture patterns resulted from triaxial tests on 25 mm diameter samples at different confining pressures.

References

Andreev, G.E., 1991a. A review of the Brazilian test for rock tensile strength determination. Part I: calculation formula. Min. Sci. Technol. 13, 445–456.

Andreev, G.E., 1991b. A review of the Brazilian test for rock tensile strength determination. Part II: contact conditions. Min. Sci. Technol. 13.

Andresen, B., Salamon, P.R.B., 1984. Thermodynamics in finite time. Phys. Today 37, 62–70.

ASTM, 2000. American Society for Testing and Materials, Annual Book of ASTM Standards, Philadeplhia, PA, USA.

Aubertin, M., Li, L., Simon, R., 2000. A multiaxial stress criterion for short and long term strength of isotropic rock media. Int. J. Rock Mech. Min. Sci. 37, 1169–1193.

Baecher, G.B., Einstein, H.H., 1981. Size effect in rock testing. Geophys. Res. Lett. 8, 671–674.

Bahaaddini, M., Hagan, P.C., Mitra, R., Hebblewhite, B.K., 2014. Scale effect on the shear behaviour of rock joints based on a numerical study. Eng. Geol. 181, 212–223.

Bandis, S., 1980. Experimental Studies of Scale Effects on Shear Strength and Deformation of Rock Joints. Department of Earth Sciences. The University of Leeds.

Bandis, S., Lumsden, A.C., Barton, N.R., 1981. Experimental studies of scale effects on the shear behaviour of rock joints. Int. J. Rock Mech. Min. Sci. Geomech. Abstr. 18, 1–21.

Barton, N., Bandis, S., 1982. Effects of Block Size on the Shear Behavior of Jointed Rock. American Rock Mechanics Association.

Baud, P., Reuschle, T., Ji, Y., Cheung, C.S.N., Wong, T.-F., 2015. Mechanical compaction and strain localization in Bleurswiller sandstone. J. Geophys. Res. Solid Earth. http://dx.doi.org/10.1002/2015JB012192. Accepted manuscript.

Baud, P., Zhu, W., Wong, T.F., 2000. Failure mode and weakening effect of water on sandstone. J. Geophys. R. 105, 16371–16389.

Bésuelle, P., Desrues, J., Raynaud, S., 2000. Experimental characterisation of the localisation phenomenon inside a Vosges sandstone in a triaxial cell. Int. J. Rock Mech. Min. Sci. 37, 1223–1237.

Brady, B.H.G., Brown, E.T., 2006. Rock Mechanics for Underground Mining. Springer, Dordrecht, Netherlands.

Brantut, N., Heap, M.J., Baud, P., Meredith, P.G., 2014. Rate- and strain-dependent brittle deformation of rocks. J. Geophys. Res. Solid Earth 119, 1818–1836.

Broch, E., Franklin, J.A., 1972. The point-load strength test. Int. J. Rock Mech. Min. Sci. 9, 669–697.

Brook, N., 1980. Size correction for point load testing. Int. J. Rock Mech. Min. Sci. 17, 231–235.

Butenuth, C., 1997. Comparison of tensile strength values of rocks determined by point load and direct tension tests. Rock Mech. Rock Eng. 30, 65–72.

Byerlee, J., 1967. Frictional characteristics of granite under high confining pressure. J. Geophys. Res. 72, 3639–3648.

Byerlee, J., 1978. Friction of rocks. PAGEOPH 116, 615–626.

Çanakcia, H., Pala, M., 2007. Tensile strength of basalt from a neural network. Eng. Geol. 94, 10–18.

Carpenter, B.M., Marone, C., Saffer, D.M., 2011. Weakness of the San Andreas Fault revealed by samples from the active fault zone. Nat. Geosci. 4, 251–254.

Carpenter, B.M., Saffer, D.M., Marone, C., 2015. Frictional properties of the active San Andreas Fault at SAFOD: implications for fault strength and slip behavior. J. Geophys. Res. Solid Earth 120, 5273–5289.

Carpinteri, A., Chiaia, B., Ferro, G., 1995. Size effects on nominal tensile strength of concrete structures: multifractality of material ligaments and dimensional transition from order to disorder. Mat. Struct. 28, 311–317.

Carpinteri, A., Paggi, M., 2005. Size-scale effects on the friction coefficient. Int. J. Solids Struct. 42, 2901–2910.

Chang, N.Y., Jumper, A.L., 1978. Multiple-stage Triaxial Test on Oil Shale. American Rock Mechanics Association, Reno, Nevada.

Crider, J.G., Peacock, D.C.P., 2004. Initiation of brittle faults in the upper crust: a review of field observations. J. Struct. Geol. 26, 691–707.

Darlington, W.J., Ranjith, P.G., 2011. The effect of specimen size on strength and other properties in laboratory testing of rock and rock-like cementitious brittle materials. Rock Mech. Rock Eng. 44, 513–529.

Desrues, J., Andò, E., 2015. Strain localisation in granular media. Comptes Rendus Phys. 16, 26–36.

Durrleman, S., Boschetti, F., Ord, A., Regenauer-Lieb, K., 2006. Automatic detection of particle aggregation in particle code simulations of rock deformation. Geochem. Geophys. Geosys. 7 n/a-n/a.

Edmond, J.M., Paterson, M.S., 1972. Volume changes during the deformation of rocks at high pressures. Int. J. Rock Mech. Min. Sci. 9, 161–182.

El Bied, A., Sulem, J., Martineau, F., 2002. Microstructure of shear zones in Fontainebleau sandstone. Int. J. Rock Mech. Min. Sci. 39, 917–932.

Elices, M., Rocco, C., 1999. Size effect and boundary conditions in Brazilian test: theoretical analysis. J. Mater. Struct. 32, 437–444.

Elliot, G.M., Brown, E.T., 1985. Yield of soft, high porosity rock. Geotechnique 35, 413–423.

Forbes, M., Masoumi, H., Saydam, S., Hagan, P., 2015. Investigation into the effect of length to diameter ratio on the point load strength index of Gosford sandstone. In: 49th US Rock Mechanics/Geomechanics Symposium. American Rock Mechanics Association, San Francisco, US, pp. 478–488, 28 June- 1 July.

Francois, B., Lacombe, F., Herrmann, H.J., 2002. Finite width of shear zones. Phys. Rev. E 65, 031311.

Geers, M.G.D., Kouznetsova, V.G., Brekelmans, W.A.M., 2010. Multi-scale computational homogenization: trends and challenges. J. Comput. Appl. Math. 234, 2175–2182.

Greminger, M., 1982. Experimental studies of the influence of rock anisotropy and size and shape effects in point-load testing. Int. J. Rock Mech. Min. Sci. 19, 241–246.

Hawkins, A.B., 1998. Aspects of rock strength. Bull. Eng. Geol. Env. 57, 17–30.

Hunt, D.D., 1973. The Influence of Confining Pressure on Size Effect. Massachusetts Institute of Technology, USA.

ISRM, 2007. The complete suggested methods for rock characterization, testing and monitoring: 1974–2006 ISRM. In: Ulusay, R., Hudson, J.A. (Eds.), Suggested Methods Prepared by the Commission on Testing Methods, Compilation Arranged by the ISRM Turkish National Group. Kozan ofset, Ankara.

Khan, A.S., Xiang, Y., Huang, S., 1991. Behaviour of Berea sandstone under confining pressure part I: yield and failure surfaces and nonlinear elastic response. Int. J. Plast. 7, 607–624.

Khan, A.S., Xiang, Y., Huang, S., 1992. Behaviour of Berea sandstone under confining pressure part II: elastic-plastic response. Int. J. Plast. 8, 209–230.

Klein, E., Baud, P., Reuschle, T., Wong, T.F., 2001. Mechanical behaviour and failure mode of Bentheim sandstone under triaxial compression. Phys. Chem. Earth 26, 21–25.
Kohli, A.H., Zoback, M.D., 2013. Frictional properties of shale reservoir rocks. J. Geophys. Res. Solid Earth 118, 5109–5125.
Liu, J., Freij-Ayoub, R., Regenauer-Lieb, K., 2015. Rock plasticity from micro-tomography and upscaling. J. Earth Sci. 26, 53–59.
Masoumi, H., Bahaaddini, M., Kim, G., Hagan, P., 2014. Experimental investigation into the mechanical behavior of Gosford sandstone at different sizes. In: 8th US Rock Mechanics/Geomechanics Symposium. ARMA, US, Minnesota, pp. 1210–1215.
Masoumi, H., Saydam, S., Hagan, P.C., 2016. Unified size-effect law for intact rock. Int. J. Geomech. 16, 04015059.
Maurer, W.C., 1965. Shear failure of rock under compression. SPE J. 5.
Medhurst, T.P., Brown, E.T., 1998. A study of the mechanical behaviour of coal for pillar design. Int. J. Rock Mech. Min. Sci. 35, 1087–1105.
Mogi, K., 1962. The influence of dimensions of specimens on the fracture strength of rocks. Bull. Earth Res. Inst. 40, 175–185.
Mogi, K., 1966. Pressure Dependence Rock Strength and Transition from Brittle Fracture to Ductile Flow, vol. 44. Bulletin, Earthquake Research Institute, Tokyo University, pp. 4741–4750.
Mühlhaus, H.B., Vardoulakis, I., 1987. The thickness of shear bands in granular materials. Géotechnique 37, 271–283.
Niandou, H., Shao, J.F., Henry, J.P., Fourmaintraux, D., 1997. Laboratory investigation of the mechanical behaviour of Tournemire shale. Int. J. Rock Mech. Min. Sci. 34, 3–16.
Ord, A., 1990. Mechanical Controls on Dilatant Shear Zones, vol. 54. Geological Society, London, pp. 183–192. Special Publications.
Ord, A., Hobbs, B., Regenauer-Lieb, K., 2007. Shear band emergence in granular materials—a numerical study. Int. J. Numer. Anal. Methods Geomech. 31, 373–393.
Ord, A., Vardoulakis, I., Kajewski, R., 1991. Shear band formation in gosford sandstone. Int. J. Rock Mech. Min. Sci. 28, 397–409.
Panek, L.A., Fannon, T.A., 1992. Size and shape effects in point load tests of irregular rock fragments. Rock Mech. Rock Eng. 25, 109–140.
Parry, R.H.G., 1960. Triaxial compression and extension tests on remoulded saturated clay. Géotechnique 10, 166–180.
Poliakov, A.B., Herrmann, H.J., Podladchikov, Y.Y., Roux, S., 1994. Fractal plastic shear bands. Fractals 02, 567–581.
Pratt, H.R., Black, A.D., Brown, W.S., Brace, W.F., 1972. The effect of specimen size on the mechanical properties of unjointed diorite. Int. J. Rock Mech. Min. Sci. 9, 513–529.
Regenauer-Lieb, K., Karrech, A., Chua, H.T., Poulet, T., Veveakis, M., Wellmann, F., Liu, J., Schrank, C., Gaede, O., Trefry, M.G., Ord, A., Hobbs, B., Metcalfe, G., Lester, D., 2014. Entropic bounds for multi-scale and multi-physics coupling in earth sciences. In: Dewar, C.R., Lineweaver, H.C., Niven, K.R., Regenauer-Lieb, K. (Eds.), Beyond the Second Law: Entropy Production and Non-equilibrium Systems. Springer Berlin Heidelberg, Berlin, Heidelberg, pp. 323–335.
Regenauer-Lieb, K., Poulet, T., Veveakis, M., 2016. A novel wave-mechanics approach for fluid flow in unconventional resources. Lead. Edge 35, 90–97.
Regenauer-Lieb, K., Veveakis, M., Poulet, T., Wellmann, F., Karrech, A., Liu, J., Hauser, J., Schrank, C., Gaede, O., Fusseis, F., 2013a. Multiscale coupling and multiphysics approaches in earth sciences: Applications. J. Coupled Syst. Multiscale Dyn. 1.
Regenauer-Lieb, K., Veveakis, M., Poulet, T., Wellmann, F., Karrech, A., Liu, J., Hauser, J., Schrank, C., Gaede, O., Trefry, M., 2013b. Multiscale coupling and multiphysics approaches in earth sciences: Theory. J. Coupled Syst. Multiscale Dyn. 1, 49–73.
Regenauer-Lieb, K., Yuen, D., 2004. Positive feedback of interacting ductile faults from coupling of equation of state, rheology and thermal-mechanics. Phys. Earth Planet. Interiors 142, 113–135.
Roshan, H., Oeser, M., 2012. A non-isothermal constitutive model for chemically active elastoplastic rocks. Rock Mech. Rock Eng. 45, 361. http://dx.doi.org/10.1007/s00603-011-0204-z.
Roshan, H., Masoumi, H., Hagan, P., 2016a. On size-dependent uniaxial compressive strength of sedimentary rocks in reservoir geomechanics. In: 50th US Rock Mechanics/Geomechanics Symposium. ARMA, Houston, US.
Roshan, H., Sari, M., Arandiyan, H., Hu, Y., Mostaghimi, P., Sarmadivaleh, M., Masoumi, H., Veveakis, M., Iglauer, S., Regenauer-Lieb, K., 2016b. Total porosity of tight rocks: a welcome to heat transfer technique. Energy & Fuels. http://dx.doi.org/10.1021/acs.energyfuels.6b01339.
Schellart, W.P., 2000. Shear test results for cohesion and friction coefficients for different granular materials: scaling implications for their usage in analogue modelling. Tectonophysics 324, 1–16.
Singh, M.M., Huck, P.J., 1972. Large scale triaxial tests on rock. In: The 14th US Symposium on Rock Mechanics Penn State University, Pennsylvania, US, pp. 35–60.
Sufian, A., Russell, A.R., 2013. Microstructural pore changes and energy dissipation in Gosford sandstone during pre-failure loading using X-ray CT. Int. J. Rock Mech. Min. Sci. 57, 119–131.
Sulem, J., Ouffroukh, H., 2006a. Hydromechanical behaviour of fontainebleau sandstone. Rock Mech. Rock Eng. 39, 185–213.
Sulem, J., Ouffroukh, H., 2006b. Shear banding in drained and undrained triaxial tests on a saturated sandstone: porosity and permeability evolution. Int. J. Rock Mech. Min. Sci. 43, 292–310.
Terada, K., Hori, M., Kyoya, T., Kikuchi, N., 2000. Simulation of the multi-scale convergence in computational homogenization approaches. Int. J. Solids Struct. 37, 2285–2311.
Thuro, K., Plinninger, R.J., Zah, S., Schutz, S., 2001a. Scale Effect in Rock Strength Properties. Part 1: Unconfined Compressive Test and Brazilian Test, Rock Mechanics- a Challenge for Society. Zeitlinger, Switzerland, pp. 169–174.
Thuro, K., Plinninger, R.J., Zah, S., Schutz, S., 2001b. Scale Effect in Rock Strength Properties. Part 2: Point Load Test and Point Load Strength Index, Rock Mechanics- a Challenge for Society. Zeitlinger, Switzerland, pp. 175–180.
Vermeer, P.A., 1990. The orientation of shear bands in biaxial tests. Géotechnique 40, 223–236.
Veveakis, E., Regenauer-Lieb, K., 2015a. Cnoidal waves in solids. J. Mech. Phys. Solids 78, 231–248.
Veveakis, E., Regenauer-Lieb, K., 2015b. Review of extremum postulates. Curr. Opin. Chem. Eng. 7, 40–46.
Wasantha, P.L.P., Ranjith, P.G., Viete, D.R., 2014. Effect of joint orientation on the hydromechanical behavior of singly jointed sandstone experiencing undrained loading. J. Geophys. Res. Solid Earth 119, 1701–1717.
Wawersik, W.R., Fairhurst, C., 1970. A study of brittle rock fracture in laboratory compression experiments. Int. J. Rock Mech. Min. Sci. 7, 561–575.
Wong, T.-f., Baud, P., 2012. The brittle-ductile transition in porous rock: a review. J. Struct. Geol. 44, 25–53.
Wong, T.-f., David, C., Zhu, W., 1997. The transition from brittle faulting to cataclastic flow in porous sandstones: mechanical deformation. J. Geophys. Res. Solid Earth 102, 3009–3025.